

Dynamic Phasor Modeling of the Doubly-fed Induction Generator under Unbalanced Conditions

T. Demiray, F. Milano and G. Andersson

Abstract—This paper proposes the use of the dynamic phasor approach for studying the behavior of doubly-fed induction generators during faults and unbalanced conditions. The dynamic phasor approach provides more accurate models than the quasi-stationary ones and, at the same time, is computationally more efficient than detailed EMTP models. Two contingencies are taken as examples to study the wind turbine behavior: balanced and unbalanced voltage sags. Results are compared with standard electromechanical and electromagnetical models.

Index Terms—Dynamic phasor approach, wind turbine, doubly-fed induction generator, unbalanced condition, voltage sag.

I. INTRODUCTION

In recent years, wind power generation has become very significant in different countries around the world [1]–[3]. Due to the increasing wind power penetration, wind farms, like conventional power plants, should be considered in the future in the dynamic stability assessment of power systems.

Special rules and requirements have recently been set for wind power production, such as the behavior of wind generators during unbalanced conditions [2]. In this respect, a major concern is the response to voltage sags that occur at the bus where the wind farm is connected to the network. So far, wind farms were most often disconnected if a voltage sag of a significant magnitude occurred. However, new grid regulations impose that wind farms must contribute actively to grid stability (e.g. Spanish regulation on renewable generation [4]).

To address the wind farm adequacy with respect to contingencies, the first step is to set up an accurate model of the wind turbines. In this paper, only the variable speed wind turbine with doubly-fed induction generator (DFIG) is considered as it is the most common device used in actual wind farms [5].

Some commercial software packages are able to simulate the electromagnetical model of wind turbines (e.g. PSCAD, PLECS, Simpow, DigSilent, PSS/E, SimPowerSyms). A comparison of these models can be found in [6]. The detailed electromagnetical model is adequate for studying the behavior of a single machine, but the computational burden can become cumbersome for studying the behavior of a wind farm that is typically composed of tens of wind turbines.

T. Demiray is with Power Systems Laboratory, ETH Zürich, Zürich, Switzerland. Email: demiray@eeh.ee.ethz.ch

F. Milano is with the Department of Electrical Engineering, University of Castilla-La Mancha, 13071 Ciudad Real, Spain. E-mail: Federico.Milano@uclm.es

G. Andersson is with Power Systems Laboratory, ETH, Zürich, Switzerland. Email: andersson@eeh.ee.ethz.ch

On the other hand, electromechanical models are adequate to study the collective behavior of wind farms. A variety of simplified models for transient and voltage stability studies have been proposed in the literature [7]–[9]. However, electromechanical fundamental frequency models are not particularly suitable for studying unbalanced conditions.

This paper proposes the use of the dynamic phasor approach for modeling and studying the behavior of DFIGs. Dynamic phasors provide a suitable framework which is able to model accurately unbalanced conditions and, at the same time, is computationally more efficient than EMTP simulations. In particular, the dynamic phasors approach has been applied to model unbalanced three-phase systems with electric machines, FACTS devices and power converters [10]–[13].

Two studies are carried out to investigate the wind turbine behavior during balanced and unbalanced conditions. These cases are briefly described below:

- 1) Balanced Voltage sag near to DFIG bus.
- 2) Unbalanced Voltage sag near to DFIG bus.

The response of electromagnetical and dynamic phasor models are compared and discussed for the two cases. The electromechanical fundamental frequency model behavior is also compared for the balanced voltage sag case.

The paper is organized as follows. Section II presents the dynamic phasor approach which is used in this paper to model the induction machine and the converter of the DFIG. In Section III, starting from the detailed model equations for induction machine and converter, the proposed DFIG model is derived using the dynamic phasors approach. Section IV gives a comparative assessment of the derived models. Section V comprises simulations with the proposed dynamic phasor models and detailed models following balanced and unbalanced voltage sags. Furthermore the accuracy and efficiency of different models are compared to each other. Finally, in Section VI, conclusions are duly drawn.

II. OUTLINES OF THE DYNAMIC PHASOR APPROACH

The main idea of *Dynamic Phasor Approach*, which is used to derive the models in Section III, is to approximate a possibly complex time domain waveform $x(\tau)$ in the interval $\tau \in (t - T, t]$ with a Fourier series representation of the form

$$x(\tau) \approx \text{Re} \left\{ \sum_{k \in K} X_k(t) \cdot e^{jk\omega\tau} \right\} \quad (1)$$

$$X_k(t) = \frac{1}{T} \int_{t-T}^t x(\tau) \cdot e^{-jk\omega\tau} d\tau = \langle x \rangle_k(t) \quad (2)$$

where $\omega = 2\pi/T$ and $X_k(t)$ is the k^{th} time varying Fourier coefficient in complex form, also called *dynamic phasor*, and K is the set of selected Fourier coefficients which provide a good approximation of the original waveform (e.g. $K = \{0, 1, 2\}$).

The dynamic phasors approach offers a number of advantages over conventional methods.

- The selection of K gives a wider bandwidth in the frequency domain than traditional slow quasi-stationary models used in Transient Stability Programs.
- The selection and variation of K gives also the possibility of showing couplings between various quantities and addressing particular problems at different frequencies.
- As the variations of dynamic phasors X_k are much slower than the instantaneous quantities x , they can be used to compute the fast electromagnetic transients with larger step sizes, so that it makes simulation potentially faster than conventional time domain EMTP-like simulation.
- At steady state the dynamic phasors X_k become constant.
- The time domain simulations of such large systems with periodically switched power electronic based components have not only a fairly high computational burden, but also give little insight into the system sensitivities used to design controllers or protection schemes. The dynamic phasors approach also allows an analytical insight into such problems, as it approximates a periodically switched system with a continuous system.

Some important properties of dynamic phasors are:

- The relation between the derivatives of $x(\tau)$ and the derivatives of $X_k(t)$, which is given in (3), where the time argument t has been omitted for clarity. This can easily be verified by differentiating the formula given in (1)

$$\left\langle \frac{dx}{dt} \right\rangle_k = \frac{dX_k}{dt} - j \cdot k \cdot \omega \cdot X_k \quad (3)$$

- The product of two time-domain variables equals a discrete time convolution of the two dynamic phasor sets of variables, which is given in (4).

$$\langle x \cdot y \rangle_k = \sum_{l=-\infty}^{\infty} (X_{k-l} \cdot Y_l) \quad (4)$$

In the simulation framework used in [14], the model behavior of the power system components are normally described by the **D**ifferential **S**witched-**A**lgebraic **S**tate-**R**eset (DSAR) equations [15].

$$\begin{aligned} \frac{dx}{dt} &= f(x, y) \\ 0 &= g(x, y) \end{aligned} \quad (5)$$

Using the appropriate approximations for dynamic states x and algebraic states y in (1) and the properties (3-4), we can transform the set of f and g equations of the model into a new set of equations and get the definition of the dynamic phasor model in a new set of functions F and G as

$$\begin{aligned} \frac{dX_k}{dt} &= F_k(X_k, Y_k) - j \cdot k \cdot \omega \cdot X_k \\ 0 &= G_k(X_k, Y_k) \end{aligned} \quad (6)$$

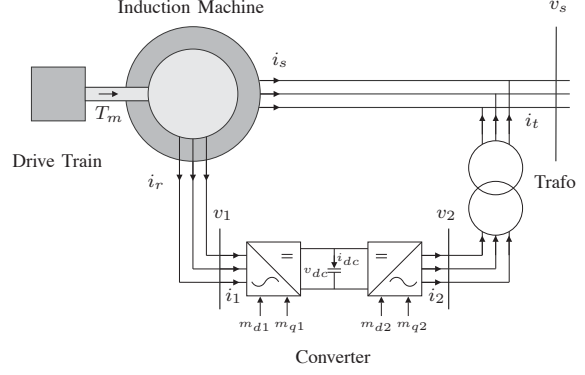


Fig. 1. Doubly-fed induction generator scheme.

where the dynamic phasors X_k become the new continuous dynamic states and Y_k the new algebraic states.

III. PROPOSED MODEL OF THE DOUBLY-FED INDUCTION GENERATOR

This section describes in detail the proposed dynamic phasor model of the doubly-fed induction generator. The DFIG is composed of a wind turbine, an induction machine, a back-to-back converter and a transformer (see Fig. 1).

A. Drive Train Model

In this paper, all rotating masses, such as turbine, gearbox and shafts, are lumped together into a single equivalent mass. Elastic shafts and resulting torques are neglected. Thus, the model behavior of the drive train is given by the simple swing equation as

$$\frac{d\omega_r}{dt} = \frac{T_m - T_e}{2H} \quad (7)$$

where T_m is the mechanical torque extracted from wind, T_e is the electrical torque produced by the induction machine and ω_r is the rotor speed (frequency). T_m is assumed to be constant in our case studies.

The dynamic phasor model equations of the drive train will be derived in the following subsection together with the induction machine equations.

B. Induction Machine

The starting point for the derivation of the dynamic phasor model of the wound rotor induction machine are the well-known model equations in the dq -reference frame rotating at synchronous speed ω_s [16].

Stator Voltage Equations:

$$\begin{aligned} \frac{d\psi_{ds}}{dt} &= v_{ds} + R_s i_{ds} + \omega_s \psi_{qs} \\ \frac{d\psi_{qs}}{dt} &= v_{qs} + R_s i_{qs} - \omega_s \psi_{ds} \end{aligned} \quad (8)$$

Rotor Voltage Equations:

$$\begin{aligned}\frac{d\psi_{dr}}{dt} &= v_{dr} + R_r i_{dr} + \sigma \omega_s \psi_{qr} \\ \frac{d\psi_{qr}}{dt} &= v_{qr} + R_r i_{qr} - \sigma \omega_s \psi_{dr}\end{aligned}\quad (9)$$

Stator and rotor flux linkage equations:

$$\begin{aligned}\psi_{ds} &= (L_s + L_m) i_{ds} + L_m i_{dr} \\ \psi_{qs} &= (L_s + L_m) i_{qs} + L_m i_{qr} \\ \psi_{dr} &= (L_r + L_m) i_{dr} + L_m i_{ds} \\ \psi_{qr} &= (L_r + L_m) i_{qr} + L_m i_{qs}\end{aligned}\quad (10)$$

Torque equation:

$$T_e = \psi_{qr} i_{dr} - \psi_{dr} i_{qr} \quad (11)$$

where in the rotor voltage equations σ is the slip of the synchronous speed ω_s and the rotor frequency ω_r and is defined as

$$\sigma = (\omega_s - \omega_r) / (\omega_s) \quad (12)$$

As stated before, the key point in the derivation of the dynamic phasor models is the appropriate selection of a set X_k in (1) for an adequate approximation of the model behavior. As *unbalanced* conditions are of concern, the system will contain not only the positive sequence quantities but also negative sequence quantities. After Park's (dq0) transformation, the fundamental frequency ac quantities in positive and negative sequence are respectively mapped as dc and second harmonic values in dq -reference frame. Due to this fact, an appropriate selection for K in (1) would be $K = \{0, 2\}$ for the model derivation.

- $k = 0$ includes positive sequence quantities
- $k = 2$ includes negative sequence quantities.

The zero sequence quantities are omitted as no neutral currents are possible due to winding connections.

Using the properties for derivative (3) and product (4), and setting $\omega = \omega_s$ in (3), the dynamic phasor model equations of the induction machine become:

Stator voltage equations:

$$\begin{aligned}\frac{d\langle\psi_{ds}\rangle_k}{dt} &= \langle v_{ds}\rangle_k + R_s \langle i_{ds}\rangle_k + \omega_s \langle\psi_{qs}\rangle_k - jk\omega_s \langle\psi_{ds}\rangle_k \\ \frac{d\langle\psi_{qs}\rangle_k}{dt} &= \langle v_{qs}\rangle_k + R_s \langle i_{qs}\rangle_k - \omega_s \langle\psi_{ds}\rangle_k - jk\omega_s \langle\psi_{qs}\rangle_k\end{aligned}\quad (13)$$

Rotor Voltage Equations:

$$\begin{aligned}\frac{d\langle\psi_{dr}\rangle_k}{dt} &= \langle v_{dr}\rangle_k + R_r \langle i_{dr}\rangle_k + \omega_s \langle\sigma\psi_{qr}\rangle_k - jk\omega_s \langle\psi_{dr}\rangle_k \\ \frac{d\langle\psi_{qr}\rangle_k}{dt} &= \langle v_{qr}\rangle_k + R_r \langle i_{qr}\rangle_k - \omega_s \langle\sigma\psi_{dr}\rangle_k - jk\omega_s \langle\psi_{qr}\rangle_k\end{aligned}\quad (14)$$

Stator and rotor flux linkage equations:

$$\begin{aligned}\langle\psi_{ds}\rangle_k &= (L_s + L_m) \langle i_{ds}\rangle_k + L_m \langle i_{dr}\rangle_k \\ \langle\psi_{qs}\rangle_k &= (L_s + L_m) \langle i_{qs}\rangle_k + L_m \langle i_{qr}\rangle_k \\ \langle\psi_{dr}\rangle_k &= (L_r + L_m) \langle i_{dr}\rangle_k + L_m \langle i_{ds}\rangle_k \\ \langle\psi_{qr}\rangle_k &= (L_r + L_m) \langle i_{qr}\rangle_k + L_m \langle i_{qs}\rangle_k\end{aligned}\quad (15)$$

Torque and slip equation:

$$\begin{aligned}\langle T_e \rangle_k &= \langle\psi_{qr} \cdot i_{dr}\rangle_k - \langle\psi_{dr} \cdot i_{qr}\rangle_k \\ \langle \sigma \rangle_k &= (\omega_s - \langle\omega_r\rangle_k) / (\omega_s)\end{aligned}\quad (16)$$

where $k \in K$ with $K = \{0, 2\}$.

Due to the same reason, the dynamic phasor model of the drive train is given as:

$$\frac{d\langle\omega_r\rangle_k}{dt} = \frac{\langle T_m \rangle_k - \langle T_e \rangle_k}{2H} - jk\omega_s \langle\omega_r\rangle_k \quad (17)$$

again with $K = \{0, 2\}$. As the mechanical torque T_m is assumed to be constant, we have only $\langle T_m \rangle_0$ (i.e. $\langle T_m \rangle_2 = 0$).

C. Converter Model

The converter model depicted in Fig.1 consists of two PWM modulated three-legged Voltage Source Converters (VSC) connected through a dc link. In this work an average model of the VSC is used. This assumption is acceptable, since the PWM modulation frequency is much higher than the system frequency, so that the switching dynamics can be neglected. With these assumptions, the average VSC model is given by

$$\begin{aligned}v_{d(1,2)} &= m_{d(1,2)} \cdot v_{dc} \\ v_{q(1,2)} &= m_{q(1,2)} \cdot v_{dc}\end{aligned}\quad (18)$$

where m_d and m_q denote the modulation indices of the PWM. Furthermore, assuming that we have a lossless converter and a lossless dc-link, the converter dynamics can be described by the following equation.

$$\begin{aligned}\frac{dv_{dc}}{dt} &= \frac{1}{C} i_{dc} = \frac{1}{C} \left(\frac{P_1 - P_2}{v_{dc}} \right) \\ &= \frac{1}{C} (m_{d1} i_{d1} + m_{q1} i_{q1} - m_{d2} i_{d2} - m_{q2} i_{q2})\end{aligned}\quad (19)$$

If the dc-link capacitor dynamics are neglected in (19), then the equation becomes the active power balance between rotor and grid side.

Unbalanced conditions on the ac-side, give rise to oscillations with double system frequency on the dc-side. Thus, an appropriate selection for K in (1) is $K = \{0, 2\}$

- $k = 0$ for dc-quantities.
- $k = 2$ for the second harmonic due to the unbalanced conditions on the ac-side.

The dynamic phasor model of the converter is given as:

$$\begin{aligned}\frac{d\langle v_{dc} \rangle_k}{dt} &= \frac{1}{C} (\langle m_{d1} i_{d1} \rangle_k + \langle m_{q1} i_{q1} \rangle_k) \\ &\quad - \frac{1}{C} (\langle m_{d2} i_{d2} \rangle_k + \langle m_{q2} i_{q2} \rangle_k) - jk\omega_s \langle v_{dc} \rangle_k\end{aligned}\quad (20)$$

The rotor-side and grid-side controllers of the converter are standard PI controllers. The rotor-side controller (m_{d1}, m_{q1}) regulates the total active (P_g) and reactive power (Q_g) generated by the DFIG. The grid-side controller (m_{d2}, m_{q2}) regulates the dc-side voltage v_{dc} and the q -component of the grid-side current i_{2q} .

D. Transformer model

The transformer model used here in our case studies, is the constant impedance (RL) model. The model equations of the transformer in the dq reference frame rotating with ω_s are:

$$\begin{aligned} L \frac{di_d}{dt} &= v_{1d} - v_{2d} - R i_d + \omega_s L i_q \\ L \frac{di_q}{dt} &= v_{1q} - v_{2q} - R i_q - \omega_s L i_d \end{aligned} \quad (21)$$

The dynamic phasor model of the transformer is given as:

$$\begin{aligned} L \frac{d\langle i_d \rangle_k}{dt} &= \langle v_{1d} \rangle_k - \langle v_{2d} \rangle_k - R \langle i_d \rangle_k + \omega_s L \langle i_q \rangle_k \\ &\quad - jk\omega_s L \langle i_d \rangle_k \\ L \frac{d\langle i_q \rangle_k}{dt} &= \langle v_{1q} \rangle_k - \langle v_{2q} \rangle_k - R \langle i_q \rangle_k + \omega_s L \langle i_d \rangle_k \\ &\quad - jk\omega_s L \langle i_q \rangle_k \end{aligned} \quad (22)$$

IV. COMPARATIVE ASSESSMENT OF MODELS

In the case studies, four different models are compared during balanced and unbalanced voltage sags, where two of them are based on the dynamic phasors approach. These four different models are as follows:

- Detailed Models
- Fundamental Frequency Models
- Dynamic Phasor Models
- Reduced Order Dynamic Phasor Models

A. Detailed Models

Detailed Models are used in Electromagnetic Transients Programs and capture both fast dynamics due to the electromagnetic transients and slow dynamics due to electromechanical transients. The induction machine equations (7-12) capture both fast and slow dynamics. The average converter model (18-19) takes the electromagnetic dc-link dynamics into account but neglects the switching dynamics of the VSC. The transformer model (21) captures the electromagnetic transients in the transmission network.

B. Fundamental Frequency Models

Fundamental Frequency Models are most often used in Transient Stability Programs. These models neglect the electromagnetic transients, and capture only slow dynamics due to electromechanical transients. In the case of the induction machine, it is assumed that the fast electromagnetic transients in the stator windings have decayed and stator fluxes have reached their steady state values. This is achieved by setting $d/dt = 0$ in (8). The rotor flux transients (9) are still considered. For the converter, the dc-link dynamics are neglected by setting $d/dt = 0$ in (19) and the steady state value of dc-capacitor voltage is used. The same holds also for the transformer model.

We should mention that setting $d/dt = 0$ in (8), (19) and (21) is equivalent to omitting negative sequence quantities. Thus, these fundamental frequency models can only be used to simulate balanced conditions with symmetrical components, as they consider only the positive sequence quantities.

C. Dynamic Phasor Models

Dynamic Phasor Models also capture both electromagnetic and electromechanical transients as the *detailed models*. But this time we don't simulate the instantaneous values of the system quantities $x(t)$, but their time-varying Fourier coefficients (dynamic phasors) $\langle x(t) \rangle_k$. The dynamic phasor model equations of the induction machine are given in (13-17), of the converter in (20) and of the transformer (22) with $K = \{0, 2\}$.

D. Reduced Order Dynamic Phasor Models

Reduced Order Dynamic Phasor Models capture only the electromechanical transients. Stator flux electromagnetic transients of the induction machine are neglected by setting $d/dt = 0$ in (13). The dc-link dynamics of the converter and the electromagnetic transients in the transmission system are also omitted by setting $d/dt = 0$ in (20) and (22).

In contrast to fundamental frequency models, setting $d/dt = 0$ in (13),(20) and (22) means only neglecting the dynamics of positive and negative sequence quantities. These models can still be used for unbalanced conditions and even for asymmetrical components, as they include positive ($k = 0$) and negative ($k = 2$) sequence quantities.

V. SIMULATIONS

The accuracy and efficiency of the described models under balanced and unbalanced conditions are compared in the following case study. The test case under consideration is depicted in Figure 2. It consists of one DFIG connected to an external grid through a transformer. The external grid is represented as a constant voltage source, which can supply balanced and unbalanced voltages in three-phases (abc). The per unit parameters of the system are given in Appendix A. Simulations were obtained using Matlab 7.1 running on a Intel Pentium IV CPU with 3.80 GHz and 2 GB of RAM.

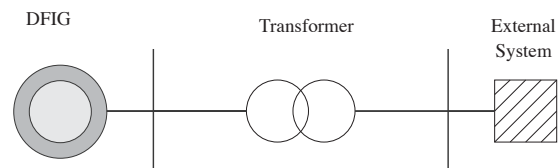
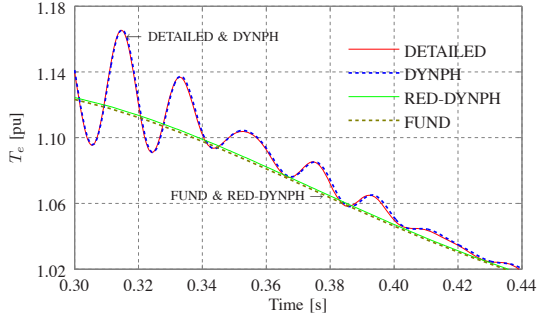
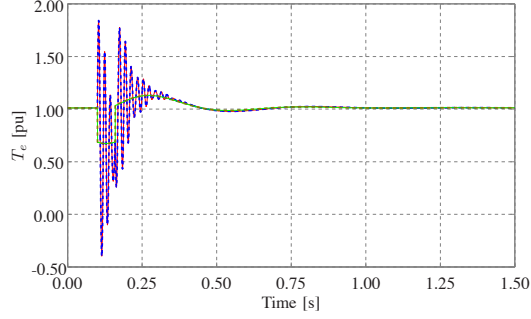


Fig. 2. Test case.

A. Simulation of Balanced Voltage Sag

In this case study, a 50% three-phase voltage sag is applied at 0.1 seconds and cleared after 3 cycles. The efficiency and the accuracy of the 4 different models are examined. Figure 3 depicts the trajectory of the machine electrical torque T_e with all 4 models. Figure 3 also shows the required cpu simulation times. A fair comparison can be drawn only between *Detailed Models* and *Dynamic Phasor Models* as they both consider electromagnetic transients, and between *Fundamental Frequency Models* and *Reduced Order Dynamic Phasor Models* as they both neglect electromagnetic transients.



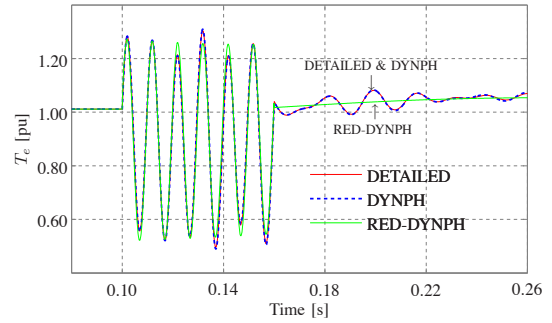
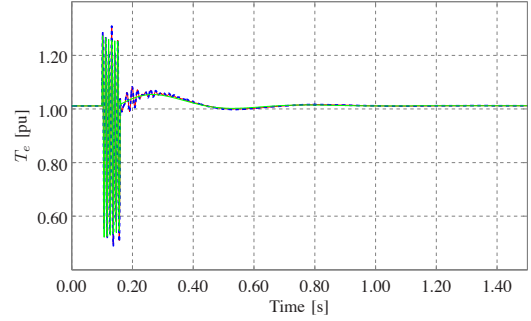
CPU SIMULATION TIMES			
DETAILED	DYNPH	FUND	RED-DYNPH
8.56 [s]	3.67 [s]	0.65 [s]	0.73 [s]

Fig. 3. 50% Balanced Voltage Sag for 3 cycles - Full simulation, zoomed section and cpu simulation times.

Figure 3 depicts a zoomed section of the overall simulation, where we see a good overall match between the results with detailed models (DETAILED) and dynamic phasor models (DYNPH). The same holds also for fundamental frequency models (FUND) and reduced order dynamic phasor models (RED-DYNPH). In DETAILED and DYNPH, we observe the decaying oscillations due to electromagnetic transients, where in FUND and RED-DYNPH these are absent as they are neglected. If cpu simulation times in Figure 3 are compared, the dynamic phasor models show a better performance than the detailed models. Even though the dynamic phasor models have 3 times more variables and equations [$\langle x \rangle_0$, $Re(\langle x \rangle_2)$, $Im(\langle x \rangle_2)$] than the detailed models, they show a higher simulation performance, as the variations in the dynamic phasors $\langle x \rangle_k$ are much slower than in the instantaneous values x . This leads to shorter simulation times whilst retaining the same degree of accuracy. Fundamental frequency models and reduced order dynamic phasor models show similar performance regarding the accuracy and efficiency.

B. Simulation of Unbalanced Voltage Sag

In this case study, a 50% one-phase voltage sag is applied at 0.1 seconds and cleared after 3 cycles. The efficiency and the accuracy of detailed models, dynamic phasor models and reduced order dynamic phasor models are compared. In this case study fundamental frequency models are omitted. As



CPU SIMULATION TIMES		
DETAILED	DYNPH	RED-DYNPH
9.18 [s]	4.6 [s]	1.2 [s]

Fig. 4. 50% Unbalanced Voltage Sag for 3 cycles - Full simulation, zoomed section and cpu simulation times.

mentioned in Section IV-B, they are not suitable for simulating unbalanced conditions. Figure 4 depicts the trajectory of the machine electrical torque T_e with all three models, and shows the required cpu simulation times. Also in the unbalanced voltage sag case, an overall good match is observed between the dynamic phasor model results and detailed model results (Fig 4). Again, the dynamic phasor models show better performance than the detailed models concerning cpu simulation time (see Fig. 4). As expected, the reduced order dynamic phasor models show the shortest simulation time, but the accuracy is low as fast dynamics are neglected. The zoomed section in the bottom pane of Figure 4 shows the electrical torque during the unbalanced voltage sag. We observe that the electrical torque value of the reduced order phasor dynamic model is also close to the value of the detailed model.

In contrast to fundamental frequency models, the reduced order dynamic phasor models are also able to simulate unbalanced conditions. Figure 5 shows the trajectory of the negative sequence electrical torque ($Re(\langle T_e \rangle_2)$ and $Im(\langle T_e \rangle_2)$).

VI. CONCLUSIONS

In this paper a dynamic phasor model of the doubly-fed induction machine including the dc-link dynamics of the converter has been derived. Simulations show that the dynamic phasor models are as accurate as the detailed time domain models for the studied cases. If simulation times are compared,

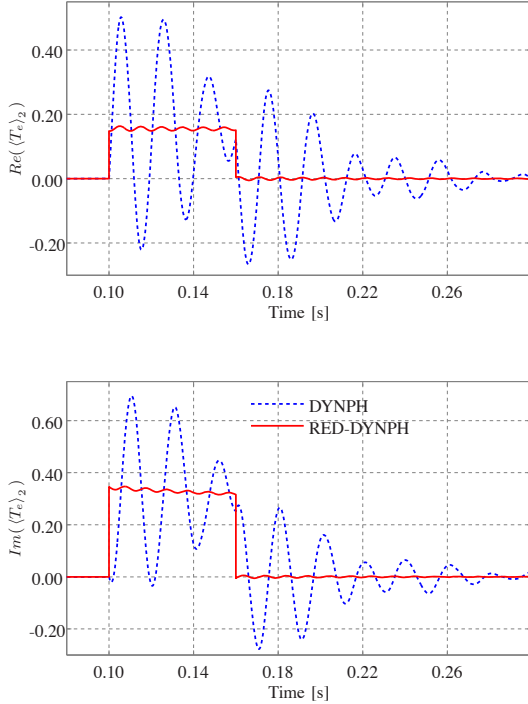


Fig. 5. 50% Unbalanced Voltage Sag - Negative Sequence Torque

the dynamic phasor models are 2-3 times faster than the detailed models.

Furthermore, reduced order dynamic phasor models are derived by neglecting the electromagnetic transients and are compared with the fundamental frequency models. The reduced order dynamic phasor models are capable of simulating unbalanced conditions, whereas fundamental frequency models can only be used for simulating balanced conditions.

Aside from its efficiency and accuracy in simulations, the dynamic phasor technique is proved to be an analytical and systematic tool for modeling and simulating power system components.

REFERENCES

- [1] E. DeMeo, W. Grant, M. R. Milligan, and M. J. Schuerger, "Wind Plant Integration: Costs, Status, and Issues," *IEEE Power & Energy Magazine*, pp. 38–46, November-December 2005.
- [2] P. B. Eriksen, T. Ackerman, H. Abildgaard, P. Smith, W. Winter, and J. Rodríguez-García, "System Operation with High Wind Penetration: The Challenges of Denmark, Germany, Spain, and Ireland," *IEEE Power & Energy Magazine*, pp. 65–74, November-December 2005.
- [3] R. Zavadil, N. Miller, A. Ellis, and E. Muljadi, "Making Connections: Wind Generation Challenges and Progress," *IEEE Power & Energy Magazine*, pp. 26–37, November-December 2005.
- [4] B. O. E., *Real Decreto 436/2004 (in Spanish)*, March 2004, available at www.boe.es.
- [5] EWEA, "Wind Force 12-A. Blueprint to Achieve 12% of the World's Electricity from Wind Power by 2020," European Wind Energy Association, Tech. Rep. 2005, 2005, available at www.ewea.org.

- [6] T. Lund, J. Eek, S. Uski, and A. Perdana, "Fault Simulation of Wind Turbines using Commercial Simulation Tools," in *Proc. Fifth International Workshop on Large-Scale Integration of Wind Power and Transmission Networks for Offshore Wind Farms*, Glasgow, 2005.
- [7] J. G. Sloopweg, S. W. H. de Haan, H. Polinder, and W. L. Kling, "General Model for representing Variable Speed Wind Turbines in Power System Dynamics Simulations," *IEEE Transactions on Power Systems*, vol. 18, no. 1, pp. 144–151, Feb. 2003.
- [8] J. G. Sloopweg, H. Polinder, and W. L. Kling, "Representing Wind Turbine Electrical Generating Systems in Fundamental Frequency Simulations," *IEEE Transactions on Power Systems*, vol. 20, no. 3, pp. 1199–1206, Aug. 2005.
- [9] R. Cano-Marín, A. Gómez-Expósito, and M. Burgos-Payán, "Wind Energy Integration in Distribution Networks: A Voltage-Stability Constrained Case Study," in *Proceedings of the VI Bulk Power System Dynamics and Control*, Cortina d'Ampezzo, Italy, Aug. 2004.
- [10] A. Stankovic and T. Aydin, "Analysis of asymmetrical faults in power systems using dynamic phasors," *Power Systems, IEEE Transactions on*, vol. 15, no. 3, pp. 1062–1068, 2000.
- [11] A. Stankovic, B. Lesieutre, and T. Aydin, "Applications of generalized averaging to synchronous and induction machines," in *North American Power Symposium*, Boston, 1996, pp. 277–282.
- [12] P. Mattavelli, G. Verghese, and A. Stankovic, "Phasor dynamics of thyristor-controlled series capacitor systems," *Power Systems, IEEE Transactions on*, vol. 12, no. 3, pp. 1259–1267, 1997.
- [13] P. C. Stefanov and A. M. Stankovic, "Modeling of upfc operation under unbalanced conditions with dynamic phasors," *Power Systems, IEEE Transactions on*, vol. 17, no. 2, p. 395, 2002.
- [14] T. Demiray and G. Andersson, "Simulation of power system dynamics using dynamic phasor models," in *SEPOPE X Paper IP-004*, Florianopolis, Brazil, 2006.
- [15] I. Hiskens and M. Pai, "Hybrid systems view of power system modelling," in *Circuits and Systems, 2000. Proceedings. ISCAS 2000 Geneva. The 2000 IEEE International Symposium on*, vol. 2, 2000, pp. 228–231 vol.2.
- [16] P. Kundur, N. J. Balu, and M. G. Lauby, *Power system stability and control*, ser. The EPRI power system engineering series. New York: McGraw-Hill, 1994.

APPENDIX A PARAMETERS OF THE TEST SYSTEM

All parameters are given on the system bases.

DFIG	Converter	TR-DFIG	TR
$f_s = 50$ [Hz]	$C = 0.5$ [pu]	$R = 0.003$ [pu]	$R = 0.015$ [pu]
$H = 3.00$ [s]		$L = 0.300$ [pu]	$L = 0.150$ [pu]
$R_s = 0.01$ [pu]	$K_{P1} = 0.0010$		
$R_r = 0.01$ [pu]	$K_{I1} = 0.0004$		
$L_s = 0.10$ [pu]	$K_{P2} = 0.0200$		
$L_r = 0.08$ [pu]	$K_{I2} = 0.0500$		
$L_m = 3.00$ [pu]			
$P_0 = 1.00$ [pu]			